

Fundamental limits on the rate of bacterial cell division

Nathan M. Belliveau^{†, 1}, Griffin Chure^{†, 2, 3}, Christina L. Hueschen⁴, Hernan G. Garcia⁵, Jane Kondev⁶, Daniel S. Fisher⁷, Julie A. Theriot^{1, 8}, Rob Phillips^{2, 9, *}

*For correspondence:

[†]These authors contributed equally to this work

¹Department of Biology, University of Washington, Seattle, WA, USA; ²Division of Biology and Biological Engineering, California Institute of Technology, Pasadena, CA, USA; ³Department of Applied Physics, California Institute of Technology, Pasadena, CA, USA; ⁴Department of Chemical Engineering, Stanford University, Stanford, CA, USA; ⁵Department of Molecular Cell Biology and Department of Physics, University of California Berkeley, Berkeley, CA, USA; ⁶Department of Physics, Brandeis University, Waltham, MA, USA; ⁷Department of Applied Physics, Stanford University, Stanford, CA, USA; ⁸Allen Institute for Cell Science, Seattle, WA, USA; ⁹Department of Physics, California Institute of Technology, Pasadena, CA, USA; *Contributed equally

Abstract This will be written next (promise).

Introduction

The observed range of bacterial growth rates is enormously diverse. In natural environments, some microbial organisms might double only once per year (*Mikucki et al., 2009*) while in comfortable laboratory conditions, growth can be rapid with several divisions per hour (*Schaechter et al., 1958*). This six order-of-magnitude difference in time scales encompasses different microbial species and lifestyles, yet even for a single species such as *E. coli*, the growth rate can be modulated over a similar scale by tuning the type and amount of nutrients in the growth medium. This remarkable flexibility in growth rate illustrates the intimate relationship between environmental conditions and the rates at which cells convert nutrients into new cellular material – a relationship that has remained a major topic of inquiry in bacterial physiology for over a century (*Jun et al., 2018*).

As was noted by Jacques Monod, “the study of the growth of bacterial cultures does not constitute a specialized subject or branch of research, it is the basic method of Microbiology.” Those words ring as true today as they did when they were written 70 years ago (*Monod, 1949*). Indeed, the study of bacterial growth has undergone a renaissance. Many of the key questions addressed by the pioneering efforts in the middle of the last century can be revisited by examining them through the lens of the increasingly refined molecular census that is available for bacteria such as the microbial workhorse *Escherichia coli*. In this work, we explore an amalgamation of recent proteomic data sets to explore fundamental limits of bacterial growth.

Several of the evergreen questions about bacterial growth that were originally raised by microbiologists in the middle of the 20th century can now be reframed in light of this newly available data. For example, what biological processes set the absolute speed limit for how fast bacterial cells can grow and reproduce? How do cells alter the absolute numbers and relative ratios of their molecular constituents as a function of changes in growth rate or nutrient availability? In this paper, we address these two questions from two distinct angles. First, as a result of an array

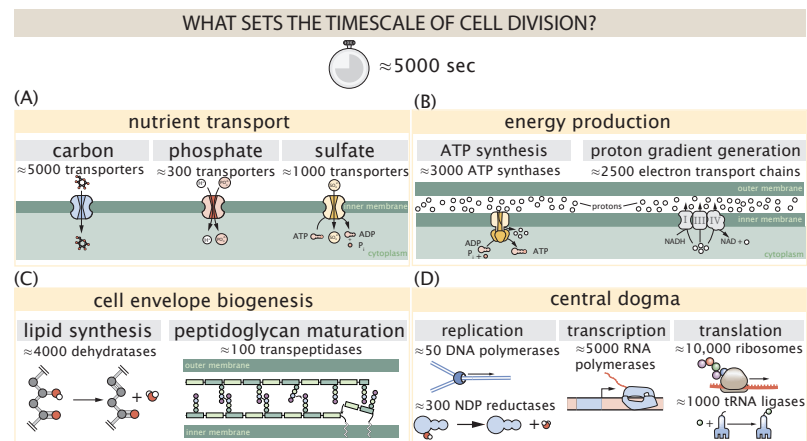


Figure 1. Transport and synthesis processes necessary for cell division. We consider an array of processes necessary for a cell to double its molecular components, broadly grouped into four classes. These categories are (A) nutrient transport across the cell membrane, (B) energy production (namely, ATP synthesis), (C) cell envelope biogenesis, and (D) processes associated with the central dogma. Numbers shown are the approximate number of complexes of each type observed at a growth rate of 0.5 hr^{-1} , or a cell doubling time of $\approx 5000 \text{ s}$.

of high-quality proteome-wide measurements of the *E. coli* proteome under myriad growth conditions, we have a census that allows us to explore how the number of key molecular players change as a function of growth rate. This census provides a window into the question of whether the rates of central processes such as energy generation or DNA synthesis are regulated systematically as a function of cell growth rate by altering protein copy number in individual cells. Second, by compiling molecular turnover rate measurements for many of the fundamental processes associated with bacterial growth, we can make quantitative estimates to determine whether the observed protein copy numbers under varying conditions appear to be in excess of what would be minimally required to support cell growth at the observed rates.

In this paper, we make a series of order-of-magnitude estimates for the copy numbers and growth rate dependent expression of a variety of different processes, schematized in **Figure 1**, informed by the collection of proteomic data sets. We use these estimates to explore which, if any, of the hypothesis illustrated in **Figure 1** may act as molecular bottlenecks that limit bacterial growth. Specifically, we leverage a combination of *E. coli* proteomic data sets collected over the past decade using either mass spectrometry (Schmidt et al., 2016; Peebo et al., 2015; Valgepea et al., 2013) or ribosomal profiling (Li et al., 2014) across 31 unique growth conditions. Throughout, our estimates we consider a modest growth rate of $\approx 0.5 \text{ hr}^{-1}$ corresponding to a doubling time of ≈ 5000 seconds, as the the data sets heavily sample this regime. While we formulate point estimates for the complex abundances at this division time, we consider how these values will vary at other growth rates due to changes in cell size, surface area, and chromosome copy number (Taheri-Araghi et al., 2015).

Broadly, we find that for the majority of these estimates the protein copy numbers appear well-tuned for the task of cell doubling at a given growth rate. From our analysis, it emerges that translation, particularly of ribosomal proteins, is the most plausible candidate for a molecular bottleneck. We reach this conclusion by considering that translation is 1) a rate limiting step for the fastest bacterial division, and 2) a major determinant of bacterial growth across the nutrient conditions we have considered under steady state, exponential growth. This enables us to suggest that the long-observed correlation between growth rate and cell size (Schaechter et al., 1958; Si et al., 2017) can be simply attributed to the increased absolute number of ribosomes per cell under conditions supporting extremely rapid growth, a hypothesis which we formally mathematize and explore.

Box 1. The Rules of Engagement for Order-Of-Magnitude Estimates

This work relies heavily on using so-called "back-of-the-envelope" estimates to understand the abundances and growth-rate dependences of a variety of molecular complexes. This moniker arises from the limitation that any estimate should be able to fit on the back of a postage envelope. As such, we must draw a set of rules governing our precision and sources of key values.

The rule of "one, few, and ten". The philosophy behind order-of-magnitude estimates is to provide a estimate of the appropriate scale, not a prediction with infinite accuracy. As such, we define three different scales of precision in making the estimates. The scale of "one" is reserved for values that range between 1 and 2. For example, If a particular process has been experimentally measured to transport 1.87 protons per second, we approximate this process to require 2 protons per event. The scale of "few" is reserved for values ranging between 3 and 5. For example, we will often use Avogadro's number to compute the number of molecules in a cell given a concentration and a volume. Rather than using Avogadro's number as 6.02214×10^{23} , we will approximate it as 5×10^{23} . Finally, the scale of "ten" is reserved for values which we know within an order of magnitude. If a particular protein complex is present at 883 copies per cell, we say that it is present in approximately 10^3 copies per cell. These different scales will be used in combination to arrive at simple estimates that report the expected scale of the observed data. Therefore, the estimates presented here should not be viewed as hard-and-fast predictions of precise copy numbers, but as approximate lower (or upper) bounds for the number of complexes that may be needed to satisfy some cellular requirement.

Furthermore, we use equality symbols ($=$) sparingly and frequently defer to approximation (\approx) or scaling (\sim) symbols when reporting an estimate. When \approx is used aside a value, we are implicitly stating that we are confident in this estimate within a factor of a few. When a scaling symbol \sim is used, we are stating that we are confident in our estimate to within an order of magnitude.

The BioNumbers Database as a source for values. In making our point estimates, we often require approximate values for key cellular properties, such as the elemental composition of the cell, the average dry mass, or approximate rates of synthesis or polymerization. We rely heavily on the BioNumbers Database (*Milo et al., 2010*) as a repository for such information. Every value we draw from the BioNumbers Database as an associated BioNumbers ID number, abbreviated as BNID. When we have used a value from the data base in making our estimate, we provide this ID number (or numbers, depending on the quantity) in parentheses on in grey-boxes in the figures. For some processes, values needed to complete the estimate were not present in the data base. In these cases, we turned to the original literature and have provided citations to the appropriate references from where the value was obtained.

Uncertainty in the data sets and the accuracy of an estimate. The data sets presented analyzed in this work are the products of extremely careful experimentation with the aim to report, to the best of their ability, the absolute copy numbers of proteins in the cell. These data, collected over the span of a few years, come from different labs and use different internal standards, controls, and even techniques. As a result, there is notable disagreement in the observed copy numbers for some complexes between the different data sets. In assessing whether our estimates could explain the observed scales and growth-rate dependencies, we considered the degree of variation between the different data sets. For example, say a particular estimate undercuts the observed data by an order of magnitude. If all data sets agree within a factor of a few of each other, we revisit our estimate and consider what we may have missed. However, if the data sets themselves disagree by an order of magnitude between them, we determine that our estimate is appropriate given the variation in the data.

Uptake of Nutrients

We begin our series of estimates by considering the critical transport processes diagrammed in **Figure 1(A)**. In order to build new cellular mass, the molecular and elemental building blocks must be scavenged from the environment in different forms. Carbon, for example, is acquired via the transport of carbohydrates and sugar alcohols with some carbon sources receiving preferential treatment in their consumption (*Monod, 1947*). Phosphorus, sulfur, and nitrogen, on the other hand, are harvested primarily in the forms of inorganic salts, namely phosphate, sulfate, and ammonia (*Jun et al., 2018; Assentoft et al., 2016; Stasi et al., 2019; Antonenko et al., 1997; Rosenberg et al., 1977; Willsky et al., 1973*). All of these compounds have different permeabilities across the cell membrane *Phillips (2018)* and most require some energetic investment either via ATP hydrolysis or through the proton electrochemical gradient to bring the material across the hydrophobic cell membrane. Given the diversity of biological transport mechanisms and the vast number of inputs needed to build a cell, we begin by considering transport of some of the most important cellular ingredients: carbon, nitrogen, oxygen, hydrogen, phosphorus, and sulfur.

The elemental composition of *E. coli* has received much quantitative attention over the past half century (*Neidhardt et al., 1991; Taymaz-Nikerel et al., 2010; Heldal et al., 1985; Bauer and Ziv, 1976*), providing us with a starting point for estimating the copy numbers of various transporters. While there is some variability in the exact elemental percentages (with different uncertainties), we can estimate that the dry mass of a typical *E. coli* cell is $\approx 45\%$ carbon (BioNumber ID: 100649, see **Box 1**), $\approx 15\%$ nitrogen (BNID: 106666), $\approx 3\%$ phosphorus (BNID: 100653), and 1% sulfur (BNID: 100655). In the coming paragraphs, we will engage in a dialogue between back-of-the-envelope estimates for the numbers of transporters needed to facilitate these chemical stoichiometries and the experimental proteomic measurements of the biological reality. Such an approach provides the opportunity to test if our biological knowledge is sufficient to understand the scale at which these complexes are produced. At the end of this section, we discuss physical limits as to the number of transporters that can be present, and comment on the plausibility of this process acting as a molecular bottleneck.

Nitrogen Transport

We must first address which elemental sources must require proteinaceous transport, meaning that the cell cannot acquire appreciable amounts simply via diffusion across the membrane. The permeability of the lipid membrane to a large number of solutes has been extensively characterized over the past century. Large, polar molecular species (such as various sugar molecules, sulfate, and phosphate) have low permeabilities while small, non-polar compounds (such as oxygen, carbon dioxide, and ammonia) can readily diffuse across the membrane. Ammonia, a primary source of nitrogen in typical laboratory conditions, has a permeability on par with water ($\sim 10^5$ nm/s, BNID:110824). In particularly nitrogen-poor conditions, *E. coli* expresses a transporter (AmtB) which appears to aid in nitrogen assimilation, though the mechanism and kinetic details of transport are still a matter of debate (*van Heeswijk et al., 2013; Khademi et al., 2004*). Beyond ammonia, another plentiful source of nitrogen come in the form of glutamate, which has its own complex metabolism and scavenging pathways. However, nitrogen is plentiful in the growth conditions examined in this work, permitting us to neglect nitrogen transport as a potential rate limiting process in cell division in typical experimental conditions. We direct the reader to the Supplemental Information for a more in-depth discussion of permeabilities and a series of calculations revealing that active nitrogen transport can be neglected for the purposes of this article.

Carbon Transport

We begin with the most abundant element in *E. coli* by mass, carbon. Using ≈ 0.3 pg as the typical *E. coli* dry mass (BNID: 103904), we estimate that $\sim 10^{10}$ carbon atoms must be brought into the cell in order to double all of the carbon-containing molecules (**Figure 2(A, top)**). Typical laboratory growth conditions, such as those explored in the aforementioned proteomic data sets, provide

carbon as a single class of sugar such as glucose, galactose, or xylose to name a few. *E. coli* has evolved myriad mechanisms by which these sugars can be transported across the cell membrane. One such mechanism of transport is via the PTS system which is a highly modular system capable of transporting a diverse range of sugars (Escalante et al., 2012). The glucose-specific component of this system transports ≈ 200 glucose molecules per second per transporter (BNID: 114686). Making the assumption that this is a typical sugar transport rate, coupled with the need to transport $\sim 10^{10}$ carbon atoms, we arrive at the conclusion that on the order of 1,000 transporters must be expressed in order to bring in enough carbon atoms to divide in 5000 s, diagrammed in the top panel of Figure 2(A). This estimate, along with the observed average number of the PTS system carbohydrate transporters present in the proteomic data sets (Schmidt et al., 2016; Peebo et al., 2015; Valgepea et al., 2013; Li et al., 2014), is shown in Figure 2(A). While we estimate 1500 transporters are needed with a 5000 s division time, we can abstract this calculation to consider any particular growth rate given knowledge of the cell density and volume as a function of growth rate and direct the reader to the Supplemental Information for more information. As revealed in Figure 2(A), experimental measurements exceed the estimate by several fold, illustrating that transport of carbon into the cell is not rate limiting for cell division. Abstracting this point estimate at 5000 s to a continuum of growth rates (grey line in Figure 2(A)) reveals an excess of transporters at other growth rates, though in rapid growth regimes, the abundance is below our simple estimate.

The estimate presented in Figure 2(A) neglects any specifics of the regulation of the carbon transport system and presents a view of how many carbohydrate transporters are present on average. Using the diverse array of growth conditions explored in the proteomic data sets, we can explore how individual carbon transport systems depend on the population growth rate. In Figure 2(B), we show the total number of carbohydrate transporters specific to different carbon sources. A striking observation, shown in the top-left plot of Figure 2(B), is the constancy in the expression of the glucose-specific transport systems. Additionally, we note that the total number of glucose-specific transporters is tightly distributed at $\approx 10^4$ per cell, the approximate number of transporters needed to sustain rapid growth of several divisions per hour. This illustrates that *E. coli* maintains a substantial number of complexes present for transporting glucose regardless of growth rate, which is known to be the preferential carbon source (Monod, 1947; Liu et al., 2005; Aidelberg et al., 2014).

It is now understood that a large number of metabolic operons are regulated with dual-input logic gates that are only expressed when glucose concentrations are low (mediated by cyclic-AMP receptor protein CRP) and the concentration of other carbon sources are elevated (Gama-Castro et al., 2016; Zhang et al., 2014b). A famed example of such dual-input regulatory logic is in the regulation of the *lac* operon which is only natively activated in the absence of glucose and the presence of allolactose, an intermediate in lactose metabolism (Jacob and Monod, 1961), though we now know of many other such examples (Ireland et al., 2020; Gama-Castro et al., 2016; Belliveau et al., 2018). This illustrates that once glucose is depleted from the environment, cells have a means to dramatically increase the abundance of the specific transporter needed to digest the next sugar that is present. Several examples of induced expression of specific carbon-source transporters are shown in Figure 2(B). Points colored in red (labeled by red text-boxes) correspond to growth conditions in which the specific carbon source (glycerol, xylose, or fructose) is present. These plots show that, in the absence of the particular carbon source, expression of the transporters is maintained on the order of $\sim 10^2$ per cell. However, when the transport substrate is present, expression is induced and the transporters become highly-expressed. The grey lines in Figure 2(B) show the estimated number of transporters needed at each growth rate to satisfy the cellular carbon requirement. It is notable that in all cases, the magnitude of induced expression (shown in red) falls close to the estimate, illustrating the ability of the cell to tune expression in response to changing environments. Together, this generic estimation and the specific examples of induced expression suggest that transport of carbon across the cell membrane, while critical for growth, is not the rate-limiting step of cell division.

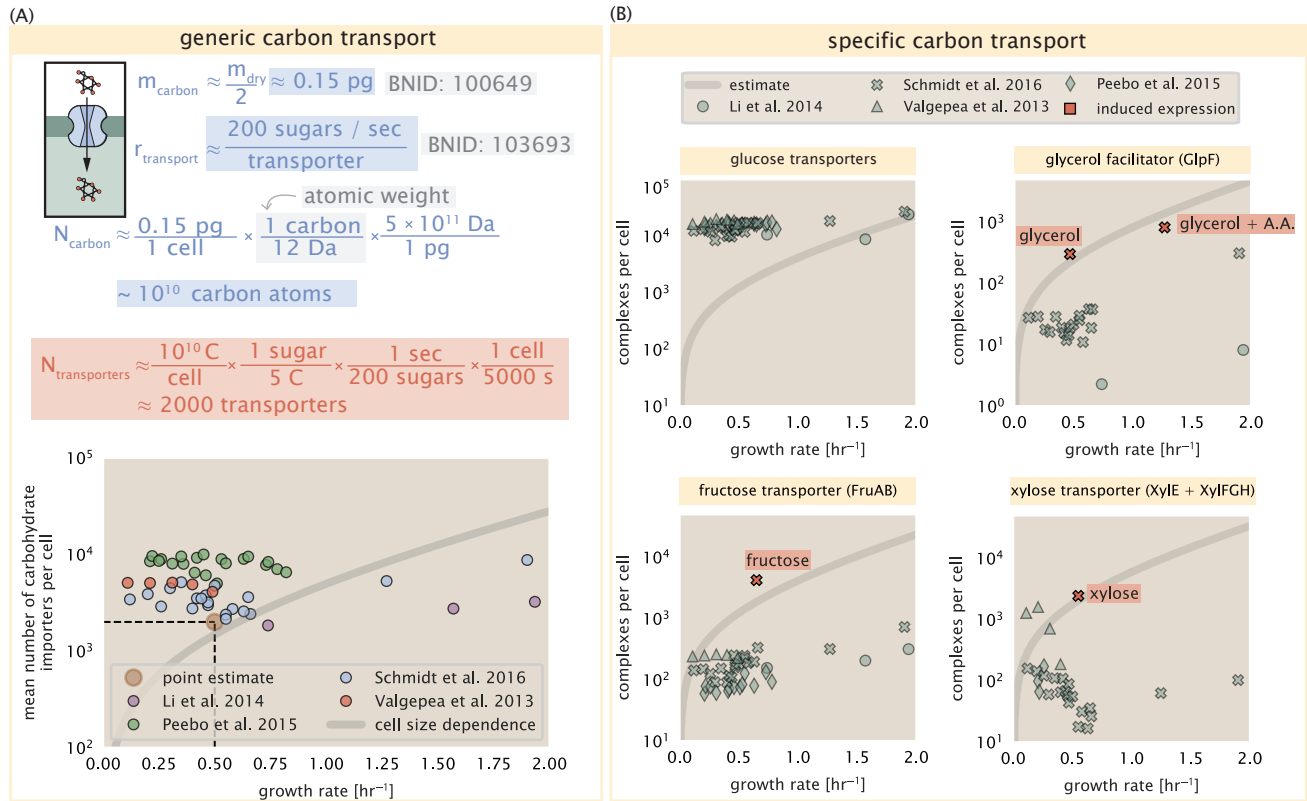


Figure 2. The abundance of carbon transport systems across growth rates. (A) A simple estimate for the minimum number of generic carbohydrate transport systems (top) assumes $\sim 10^{10}$ C are needed to complete division, each transported sugar contains ≈ 5 C, and each transporter conducts sugar molecules at a rate of ≈ 200 per second. Bottom plot shows the estimated number of transporters needed at a growth rate of ≈ 0.5 per hr (light-brown point and dashed lines). Colored points correspond to the mean number of complexes involved in carbohydrate import (complexes annotated with the Gene Ontology terms GO:0009401 and GO:0098704) for different growth conditions across different published datasets. (B) The abundance of various specific carbon transport systems plotted as a function of the population growth rate. The rates of substrate transport to compute the continuum growth rate estimate (grey line) were 200 glucose \cdot s⁻¹ (BNID: 103693), 2000 glycerol \cdot s⁻¹ (Lu et al., 2003), 200 fructose \cdot s⁻¹ (assumed to be similar to PtsI, BNID: 103693), and 50 xylose \cdot s⁻¹ (assumed to be comparable to LacY, BNID:103159). Red points and highlighted text indicate conditions in which the only source of carbon in the growth medium induces expression of the transport system. Grey line in (A) and (B) represents the estimated number of transporters per cell at a continuum of growth rates.

Phosphorus and Sulfur Transport

We now turn our attention towards other essential elements, namely phosphorus and sulfur. Phosphorus is critical to the cellular energy economy in the form of high-energy phosphodiester bonds making up DNA, RNA, and the NTP energy pool as well as playing a critical role in the post-translational modification of proteins and defining the polar-heads of lipids. In total, phosphorus makes up $\approx 3\%$ of the cellular dry mass which in typical experimental conditions is in the form of inorganic phosphate. The cell membrane has remarkably low permeability to this highly-charged and critical molecule, therefore requiring the expression of active transport systems. In *E. coli*, the proton electrochemical gradient across the inner membrane is leveraged to transport inorganic phosphate into the cell (Rosenberg *et al.*, 1977). Proton-solute symporters are widespread in *E. coli* (Ramos and Kaback, 1977; Booth *et al.*, 1979) and can have rapid transport rates of 50 to 100 molecules per second for sugars and other solutes (BNID: 103159; 111777). As a more extreme example, the proton transporters in the F_1F_0 ATP synthase, which use the proton electrochemical gradient for rotational motion, can shuttle protons across the membrane at a rate of ≈ 1000 per second (BNID: 104890; 103390). In *E. coli* the PitA phosphate transport system has been shown to be very tightly coupled with the proton electrochemical gradient with a 1:1 proton:phosphate stoichiometric ratio (Harris *et al.*, 2001; Feist *et al.*, 2007). Taking the geometric mean of the aforementioned estimates gives a plausible rate of phosphate transport on the order of 300 per second. Illustrated in Figure 3(A), we can estimate that ≈ 200 phosphate transporters are necessary to maintain an $\approx 3\%$ dry mass with a 5000 s division time. This estimate is consistent with observation when we examine the observed copy numbers of PitA in proteomic data sets (plot in Figure 3(A)). While our estimate is very much in line with the observed numbers, we emphasize that this is likely a slight overestimate of the number of transporters needed as there are other phosphorous scavenging systems, such as the ATP-dependent phosphate transporter Pst system which we have neglected.

Satisfied that there are a sufficient number of phosphate transporters present in the cell, we now turn to sulfur transport as another potentially rate limiting process. Similar to phosphate, sulfate is highly-charged and not particularly membrane permeable, requiring active transport. While there exists a H⁺/sulfate symporter in *E. coli*, it is in relatively low abundance and is not well characterized (Zhang *et al.*, 2014a). Sulfate is predominantly acquired via the ATP-dependent ABC transporter CysUWA system which also plays an important role in selenium transport (Sekowska *et al.*, 2000; Sirko *et al.*, 1995). While specific kinetic details of this transport system are not readily available, generic ATP transport systems in prokaryotes transport on the order of 1 to 10 molecules per second (BNID: 109035). Combining this generic transport rate, measurement of sulfur comprising 1% of dry mass, and a 5000 second division time yields an estimate of ≈ 1000 CysUWA complexes per cell (Figure 3(B)). Once again, this estimate is in notable agreement with proteomic data sets, suggesting that there are sufficient transporters present to acquire the necessary sulfur. In a similar spirit of our estimate of phosphorus transport, we emphasize that this is likely an overestimate of the number of necessary transporters as we have neglected other sulfur scavenging systems that are in lower abundance.

Limits on Transporter Expression

So which, if any, of these processes may be rate limiting for growth? As suggested by Figure 2 (B), induced expression can lead to an order-of-magnitude (or more) increase in the amount of transporters needed to facilitate transport. Thus, if acquisition of nutrients was the limiting state in cell division, could expression simply be increased to accommodate faster growth? A way to approach this question is to compute the amount of space in the bacterial membrane that could be occupied by nutrient transporters. Considering a rule-of-thumb for the surface area of *E. coli* of about $5 \mu\text{m}^2$ (BNID: 101792), we expect an areal density for 1000 transporters to be approximately 200 transporters/ μm^2 . For a typical transporter occupying about $50 \text{ nm}^2/\text{dimer}$, this amounts to about only 1 percent of the total inner membrane (Szenk *et al.*, 2017). In addition, bacterial cell membranes typically have densities of 10^5 proteins/ μm^2 (Phillips, 2018), implying that the cell could

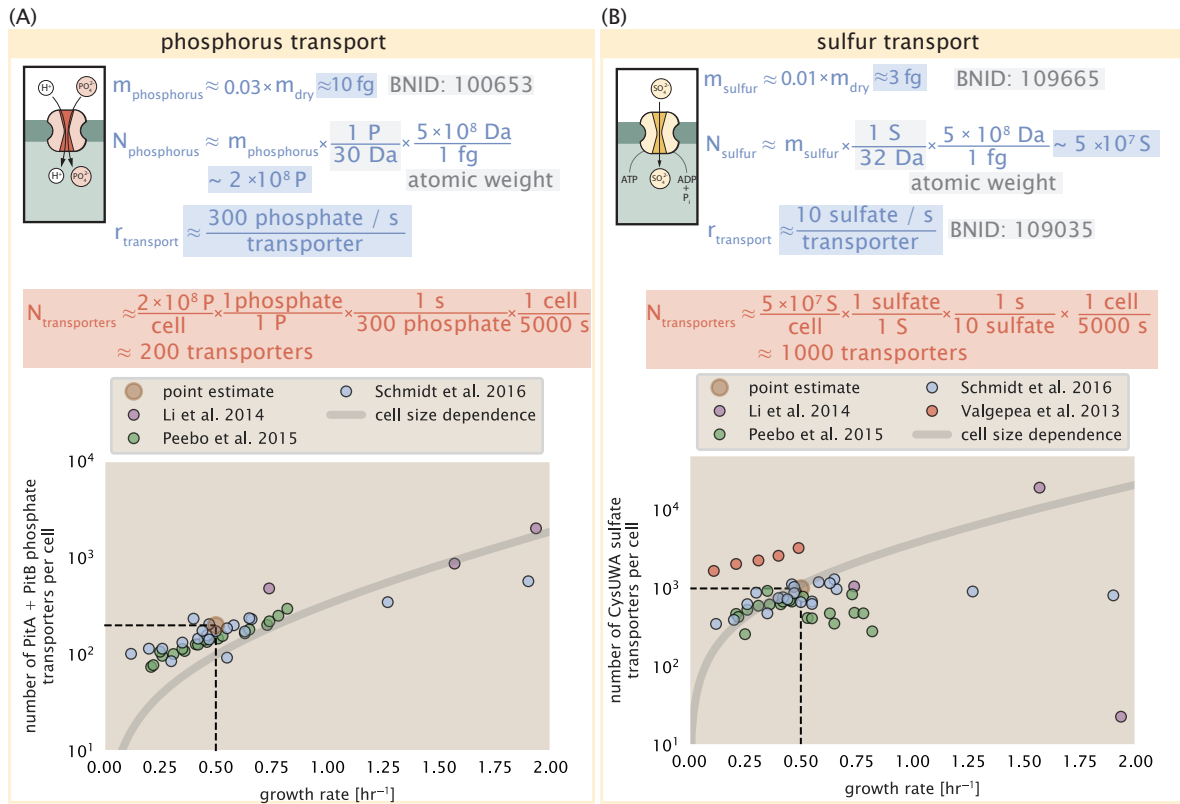


Figure 3. Estimates and measurements of phosphate and sulfate transport systems as a function of growth rate. (A) Estimate for the number of PitA phosphate transport systems needed to maintain a 3% phosphorus *E. coli* dry mass. Points in plot correspond to the the total number of PitA transporters per cell. (B) Estimate of the number of CysUWA complexes necessary to maintain a 1% sulfur *E. coli* dry mass. Points in plot correspond to average number of CysUWA transporter complexes that can be formed given the transporter stoichiometry [CysA]₂[CysU][CysW][Sbp/CysP]. Grey line in (A) and (B) represents the estimated number of transporters per cell at a continuum of growth rates.

272 accommodate more transporters of a variety of species if it were rate limiting. As we will see in the
273 next section, however, occupancy of the membrane can impose other limits on the rate of energy
274 production.

References

- Aidelberg, G., Towbin, B. D., Rothschild, D., Dekel, E., Bren, A., and Alon, U. (2014). Hierarchy of non-glucose sugars in *Escherichia coli*. *BMC Systems Biology*, 8(1):133.
- Antonenko, Y. N., Pohl, P., and Denisov, G. A. (1997). Permeation of ammonia across bilayer lipid membranes studied by ammonium ion selective microelectrodes. *Biophysical Journal*, 72(5):2187–2195.
- Assentoft, M., Kaptan, S., Schneider, H.-P., Deitmer, J. W., de Groot, B. L., and MacAulay, N. (2016). Aquaporin 4 as a NH₃ Channel. *Journal of Biological Chemistry*, 291(36):19184–19195.
- Bauer, S. and Ziv, E. (1976). Dense growth of aerobic bacteria in a bench-scale fermentor. *Biotechnology and Bioengineering*, 18(1):81–94. [_eprint: https://onlinelibrary.wiley.com/doi/pdf/10.1002/bit.260180107](https://onlinelibrary.wiley.com/doi/pdf/10.1002/bit.260180107).
- Belliveau, N. M., Barnes, S. L., Ireland, W. T., Jones, D. L., Sweredoski, M. J., Moradian, A., Hess, S., Kinney, J. B., and Phillips, R. (2018). Systematic approach for dissecting the molecular mechanisms of transcriptional regulation in bacteria. *Proceedings of the National Academy of Sciences*, 115(21):E4796–E4805.
- Booth, I. R., Mitchell, W. J., and Hamilton, W. A. (1979). Quantitative analysis of proton-linked transport systems. The lactose permease of *Escherichia coli*. *Biochemical Journal*, 182(3):687–696.
- Escalante, A., Salinas Cervantes, A., Gosset, G., and Bolívar, F. (2012). Current knowledge of the *Escherichia coli* phosphoenolpyruvate-carbohydrate phosphotransferase system: Peculiarities of regulation and impact on growth and product formation. *Applied Microbiology and Biotechnology*, 94(6):1483–1494.
- Feist, A. M., Henry, C. S., Reed, J. L., Krummenacker, M., Joyce, A. R., Karp, P. D., Broadbelt, L. J., Hatzimanikatis, V., and Palsson, B. Ø. (2007). A genome-scale metabolic reconstruction for *Escherichia coli* K-12 MG1655 that accounts for 1260 ORFs and thermodynamic information. *Molecular Systems Biology*, 3(1):121.
- Gama-Castro, S., Salgado, H., Santos-Zavaleta, A., Ledezma-Tejeda, D., Muñoz-Rascado, L., García-Sotelo, J. S., Alquicira-Hernández, K., Martínez-Flores, I., Pannier, L., Castro-Mondragón, J. A., Medina-Rivera, A., Solano-Lira, H., Bonavides-Martínez, C., Pérez-Rueda, E., Alquicira-Hernández, S., Porrón-Sotelo, L., López-Fuentes, A., Hernández-Koutoucheva, A., Moral-Chávez, V. D., Rinaldi, F., and Collado-Vides, J. (2016). RegulonDB version 9.0: High-level integration of gene regulation, coexpression, motif clustering and beyond. *Nucleic Acids Research*, 44(D1):D133–D143.
- Harris, R. M., Webb, D. C., Howitt, S. M., and Cox, G. B. (2001). Characterization of PitA and PitB from *Escherichia coli*. *Journal of Bacteriology*, 183(17):5008–5014.
- Heldal, M., Norland, S., and Tumyr, O. (1985). X-ray microanalytic method for measurement of dry matter and elemental content of individual bacteria. *Applied and Environmental Microbiology*, 50(5):1251–1257.
- Ireland, W. T., Beeler, S. M., Flores-Bautista, E., Belliveau, N. M., Sweredoski, M. J., Moradian, A., Kinney, J. B., and Phillips, R. (2020). Deciphering the regulatory genome of *Escherichia coli*, one hundred promoters at a time. *bioRxiv*.
- Jacob, F. and Monod, J. (1961). Genetic regulatory mechanisms in the synthesis of proteins. *Journal of Molecular Biology*, 3(3):318–356.
- Jun, S., Si, F., Pugatch, R., and Scott, M. (2018). Fundamental principles in bacterial physiology - history, recent progress, and the future with focus on cell size control: A review. *Reports on Progress in Physics*, 81(5):056601.
- Khademi, S., O'Connell, J., Remis, J., Robles-Colmenares, Y., Miercke, L. J. W., and Stroud, R. M. (2004). Mechanism of Ammonia Transport by Amt/MEP/Rh: Structure of AmtB at 1.35 Å. *Science*, 305(5690):1587–1594.
- Li, G.-W., Burkhardt, D., Gross, C., and Weissman, J. S. (2014). Quantifying absolute protein synthesis rates reveals principles underlying allocation of cellular resources. *Cell*, 157(3):624–635.
- Liu, M., Durfee, T., Cabrera, J. E., Zhao, K., Jin, D. J., and Blattner, F. R. (2005). Global Transcriptional Programs Reveal a Carbon Source Foraging Strategy by *Escherichia coli*. *Journal of Biological Chemistry*, 280(16):15921–15927.
- Lu, D., Grayson, P., and Schulten, K. (2003). Glycerol Conductance and Physical Asymmetry of the *Escherichia coli* Glycerol Facilitator GlpF. *Biophysical Journal*, 85(5):2977–2987.
- Mikucki, J. A., Pearson, A., Johnston, D. T., Turchyn, A. V., Farquhar, J., Schrag, D. P., Anbar, A. D., Prisco, J. C., and Lee, P. A. (2009). A Contemporary Microbially Maintained Subglacial Ferrous "Ocean". *Science*, 324(5925):397–400.

- 324 Milo, R., Jorgensen, P., Moran, U., Weber, G., and Springer, M. (2010). BioNumbers—the database of key num-
325 bers in molecular and cell biology. *Nucleic Acids Research*, 38(suppl_1):D750–D753.
- 326 Monod, J. (1947). The phenomenon of enzymatic adaptation and its bearings on problems of genetics and
327 cellular differentiation. *Growth Symposium*, 9:223–289.
- 328 Monod, J. (1949). The Growth of Bacterial Cultures. *Annual Review of Microbiology*, 3(1):371–394.
- 329 Neidhardt, F. C., Ingraham, J., and Schaechter, M. (1991). *Physiology of the Bacterial Cell - A Molecular Approach*,
330 volume 1. Elsevier.
- 331 Peebo, K., Valgepea, K., Maser, A., Nahku, R., Adamberg, K., and Vilu, R. (2015). Proteome reallocation in *Es-*
332 *cherichia coli* with increasing specific growth rate. *Molecular BioSystems*, 11(4):1184–1193.
- 333 Phillips, R. (2018). Membranes by the Numbers. In *Physics of Biological Membranes*, pages 73–105. Springer,
334 Cham, Cham.
- 335 Ramos, S. and Kaback, H. R. (1977). The relation between the electrochemical proton gradient and active trans-
336 port in *Escherichia coli* membrane vesicles. *Biochemistry*, 16(5):854–859.
- 337 Rosenberg, H., Gerdes, R. G., and Chegwidan, K. (1977). Two systems for the uptake of phosphate in *Escherichia*
338 *coli*. *Journal of Bacteriology*, 131(2):505–511.
- 339 Schaechter, M., Maaløe, O., and Kjeldgaard, N. O. (1958). Dependency on Medium and Temperature of Cell Size
340 and Chemical Composition during Balanced Growth of *Salmonella typhimurium*. *Microbiology*, 19(3):592–606.
- 341 Schmidt, A., Kochanowski, K., Vedelaar, S., Ahrné, E., Volkmer, B., Callipo, L., Knoops, K., Bauer, M., Aebersold,
342 R., and Heinemann, M. (2016). The quantitative and condition-dependent *Escherichia coli* proteome. *Nature*
343 *Biotechnology*, 34(1):104–110.
- 344 Sekowska, A., Kung, H.-F., and Danchin, A. (2000). Sulfur Metabolism in *Escherichia coli* and Related Bacteria:
345 Facts and Fiction. *Journal of Molecular Microbiology and Biotechnology*, 2(2):34.
- 346 Si, F., Li, D., Cox, S. E., Sauls, J. T., Azizi, O., Sou, C., Schwartz, A. B., Erickstad, M. J., Jun, Y., Li, X., and Jun, S. (2017).
347 Invariance of Initiation Mass and Predictability of Cell Size in *Escherichia coli*. *Current Biology*, 27(9):1278–1287.
- 348 Sirko, A., Zatyka, M., Sadowy, E., and Hulanicka, D. (1995). Sulfate and thiosulfate transport in *Escherichia coli* K-
349 12: Evidence for a functional overlapping of sulfate- and thiosulfate-binding proteins. *Journal of Bacteriology*,
350 177(14):4134–4136.
- 351 Stasi, R., Neves, H. I., and Spira, B. (2019). Phosphate uptake by the phosphonate transport system PhnCDE.
352 *BMC Microbiology*, 19.
- 353 Szenk, M., Dill, K. A., and de Graff, A. M. R. (2017). Why Do Fast-Growing Bacteria Enter Overflow Metabolism?
354 Testing the Membrane Real Estate Hypothesis. *Cell Systems*, 5(2):95–104.
- 355 Taheri-Araghi, S., Bradde, S., Sauls, J. T., Hill, N. S., Levin, P. A., Paulsson, J., Vergassola, M., and Jun, S. (2015).
356 Cell-size control and homeostasis in bacteria. - PubMed - NCBI. *Current Biology*, 25(3):385–391.
- 357 Taymaz-Nikerel, H., Borujeni, A. E., Verheijen, P. J. T., Heijnen, J. J., and van Gulik, W. M. (2010).
358 Genome-derived minimal metabolic models for *Escherichia coli* mg1655 with estimated in vivo
359 respiratory ATP stoichiometry. *Biotechnology and Bioengineering*, 107(2):369–381. _eprint:
360 <https://onlinelibrary.wiley.com/doi/pdf/10.1002/bit.22802>.
- 361 Valgepea, K., Adamberg, K., Seiman, A., and Vilu, R. (2013). *Escherichia coli* achieves faster growth by increasing
362 catalytic and translation rates of proteins. *Molecular BioSystems*, 9(9):2344.
- 363 van Heeswijk, W. C., Westerhoff, H. V., and Boogerd, F. C. (2013). Nitrogen Assimilation in *Escherichia coli*: Putting
364 Molecular Data into a Systems Perspective. *Microbiology and Molecular Biology Reviews*, 77(4):628–695.
- 365 Willsky, G. R., Bennett, R. L., and Malamy, M. H. (1973). Inorganic Phosphate Transport in *Escherichia coli*: Involvement
366 of Two Genes Which Play a Role in Alkaline Phosphatase Regulation. *Journal of Bacteriology*, 113(2):529–
367 539.
- 368 Zhang, L., Jiang, W., Nan, J., Almqvist, J., and Huang, Y. (2014a). The *Escherichia coli* CysZ is a pH dependent sulfate
369 transporter that can be inhibited by sulfite. *Biochimica et Biophysica Acta (BBA) - Biomembranes*, 1838(7):1809–
370 1816.
- 371 Zhang, Z., Aboulwafa, M., and Saier, M. H. (2014b). Regulation of crp gene expression by the catabolite repres-
372 sor/activator, cra, in *Escherichia coli*. *Journal of Molecular Microbiology and Biotechnology*, 24(3):135–141.